





# What falls versus what we recover: Quantifying search and recovery bias for orbital meteorites

Patrick M. SHOBER <sup>1,2\*</sup>, Jeremie VAUBAILLON <sup>2</sup>, Hadrien A. R. DEVILLEPOIX <sup>3,4</sup>,  
Eleanor K. SANSOM <sup>3,4</sup>, Sophie E. DEAM<sup>3,4</sup>, Simon ANGHEL<sup>2,5</sup>, Francois COLAS<sup>2</sup>,  
Pierre VERNAZZA<sup>6</sup>, and Brigitte ZANDA<sup>7</sup>

<sup>1</sup>Astromaterials Research and Exploration Science Directorate (ARES), NASA Johnson Space Center, Houston, Texas, USA

<sup>2</sup>LTE, Observatoire de Paris, Université PSL, Sorbonne Université, Université de Lille, LNE, CNRS, Paris, France

<sup>3</sup>Space Science and Technology Centre, School of Earth and Planetary Sciences, Curtin University, Perth, WA, Australia

<sup>4</sup>International Centre for Radio Astronomy Research, Curtin University, Perth, WA, Australia

<sup>5</sup>Astronomical Institute of the Romanian Academy, Bucharest, Romania

<sup>6</sup>Institut de Minéralogie, Physique des Matériaux et Cosmochimie, Muséum National d'Histoire Naturelle, CNRS, Paris, France

<sup>7</sup>Laboratoire d'Astrophysique de Marseille, Aix Marseille Université, Aix-Marseille University, CNRS, CNES, LAM, Institut Origines, Marseille, France

## \*Correspondence

Patrick M. Shober, Astromaterials Research and Exploration Science Directorate (ARES), NASA Johnson Space Center, Houston, TX, USA.

Email: [planetarypat@gmail.com](mailto:planetarypat@gmail.com)

(Received 10 March 2025; revision accepted 17 August 2025)

**Abstract**—Instrumentally determined pre-atmospheric orbits of meteorites offer crucial constraints on the provenance of extraterrestrial material and the dynamical pathways that deliver it to Earth. However, recovery efforts are focused on larger and slower impacts due to their higher survival probabilities and ease of detection. In this study, we investigate the prevalence of these biases in the population of recovered meteorites with known orbits. We compiled a data set of 75 meteorites with triangulated trajectories and compared their orbits to 538 potential > 1 g meteorite-dropping fireballs detected by the Global Fireball Observatory, the European Fireball Network, and the Fireball Recovery and InterPlanetary Observation Network. Our results reveal that objects with small semi-major axis values ( $a < 1.8$  au) appear 2–3× more often than expected. The current sample of meteorites with known orbits does not reflect the sources of meteorites in our collections, and it is essential to account for search and recovery biases to obtain a more representative understanding of meteorite source contributions.

## INTRODUCTION

Over 75,000 meteorites are cataloged in the world's collections (<https://www.lpi.usra.edu/meteor/>), with a significant proportion recovered from Antarctica (~64%). The prevalence of Antarctic meteorite finds is largely due to the unique environmental conditions that facilitate their discovery and preservation. The stark contrast between dark meteorites and the icy terrain makes visual identification more straightforward. At the same time, the cold, dry climate slows down weathering processes,

allowing meteorites to remain intact for extended periods (Corrigan et al., 2014; Harvey, 2003). Meteorites are challenging to distinguish from terrestrial rocks in most terrains on the planet, as they are often obscured by vegetation or altered by weathering. They rapidly degrade due to atmospheric and aqueous alterations, and their small size makes identification difficult. Consequently, meteorite recovery outside of hot and cold deserts is much more infrequent.

One major limitation in meteoritics is the absence of positional or spatial context for recovered meteorites.

Unlike a terrestrial geologic sample, a meteorite is not collected from an in situ outcrop on Earth where it can be placed within the planet's geological history. To address this context gap, fireball observation networks were established to monitor the night sky for the serendipitous entry of meteoroids into the Earth's atmosphere. These networks utilize arrays of cameras and sensors to detect and record fireballs—bright meteors (visual magnitude  $\leq -4$ ) produced by the ablation and fragmentation of meteoroids as they pass through the atmosphere. By capturing multiple observations of a fireball event from different locations, it is possible to reconstruct the meteoroid's pre-atmospheric orbit, providing crucial context about the impacting population (Borovička et al., 2022; Ceplecha et al., 1998; Colas et al., 2020; Devillepoix et al., 2020).

Precise trajectory data also enables the prediction of meteorite fall locations. Researchers can estimate where surviving fragments may have landed by modeling the meteoroid's final descent through the atmosphere and accounting for atmospheric winds. This facilitates targeted meteorite recovery efforts, increasing the chances of finding fresh falls with known orbital histories (Borovička, Spurný, & Brown, 2015; Jenniskens & Devillepoix, 2025). To date, over 70 meteorites (<https://www.meteoriteorbits.info/>) have been recovered with instrumentally measured orbits, and this number is growing rapidly due to advancements in observational technologies, expansion of fireball networks, and development of more advanced searching techniques (Anderson et al., 2020, 2022; Citron et al., 2021; Colas et al., 2020; Devillepoix et al., 2020). These meteorites with known trajectories offer unparalleled opportunities to study the linkage between meteoritic material and their source regions in the Solar System. With the help of these crucial data points, the source families for many meteorites have been recently identified (Brož, Vernazza, Marsset, Binzel, et al., 2024; Brož, Vernazza, Marsset, DeMeo, et al., 2024; Jenniskens & Devillepoix, 2025; Marsset et al., 2024).

Although curated meteorite collections are invaluable, the stones we recover on Earth are not pristine, in situ samples from their parent asteroids; unlike the material returned by dedicated sample-return missions such as Hayabusa, Hayabusa2, and OSIRIS-REx (Lauretta et al., 2017; Watanabe et al., 2017; Yoshikawa et al., 2015). Between the source families and our collections stand several biases and filters that affect which meteoroids ultimately become recoverable meteorites. Recent work by Shober, Devillepoix, et al. (2025) has characterized the survival bias introduced by Earth's atmosphere, a significant factor that modifies the compositional variation in our meteorite population. It has long been known that faster-moving and structurally weaker meteoroids are less likely to survive atmospheric entry due to increased

ablation and fragmentation (Ceplecha et al., 1998). However, meteoroids also undergo physical processing while in space. Collisions between meteoroids can generate smaller objects while destroying larger ones (Bottke et al., 1994; Farinella et al., 1998; Wiegert et al., 2020). Moreover, meteoroids with orbital histories at low perihelion distances also undergo significant thermal processing due to intense solar heating, which can cause them to fragment or disintegrate in space (Čapek & Vokrouhlický, 2010; Delbo et al., 2014; Granvik et al., 2016). The effects of thermal stress are well-documented among cometary populations (Bockelee-Morvan et al., 2001; Peña-Asensio et al., 2024; Rigley & Wyatt, 2022; Sekanina & Chodas, 2005, 2007, 2012; Shestakova et al., 2025); however, this process has also been recently shown to be equally important among NEAs (Cambioni et al., 2021; Delbo et al., 2014; Granvik et al., 2016; Lucchetti et al., 2024; Molaro, Walsh, et al., 2020) and even for meteoroids (Ashimbekova et al., 2025; Čapek et al., 2022; Čapek & Vokrouhlický, 2010, 2012; Shober, Devillepoix, et al., 2025). Meteoroids that have survived significant thermal processing during previous close solar approaches tend to be stronger and are more likely to survive atmospheric entry when they eventually encounter the Earth (Shober, Devillepoix, et al., 2025). These atmospheric and thermal fragmentation filters influence the flux of meteoroids reaching Earth and contribute to the observed distribution of recovered meteorites.

Even after meteoroids survive these processes and reach the ground, search and recovery practices introduce additional biases that further shape our collections. When predicting fall locations, inherent uncertainties related to the meteoroid's shape, spin, mass, and the influence of winds can result in predicted fall zones spanning several square kilometers (Towner et al., 2022). Conducting searches over such large areas is both costly and labor-intensive, necessitating the optimization of search efforts toward events with the highest likelihood of recovery. This optimization introduces potential biases into the observed orbital distribution of recovered meteorites. Search efforts often prioritize larger meteoroids and slower final speeds, as they more likely survived atmospheric entry and produced recoverable fragments. This is supported analytically—the mass-velocity bias is the inevitable consequence of equations 7.1 and 7.2 of Gritsevich (2009), when considering fireballs events in the  $\ln(\alpha)-\ln(\beta)$  space of Gritsevich et al. (2011); Gritsevich et al. (2012); Sansom, Gritsevich, et al. (2019). Large, slow bodies plot at low- $\alpha$  and low- $\beta$  values, where meteorite falls are predicted and are targeted by search teams. Consequently, our sample of meteorites with known orbits will not represent the majority of the meteoroid population impacting Earth, slightly skewing our understanding of source regions and delivery mechanisms.

This study examines the search and recovery biases for meteorites with known orbits. By comparing the recovered meteorite distribution to the predicted fall distribution derived from fireball observations across three global fireball networks—the Global Fireball Observatory (GFO), the European Fireball Network (EN), and the Fireball Recovery and InterPlanetary Observation Network (FRIPON)—we aim to quantify the extent of these biases. This analysis will provide insights into how search and recovery practices influence the sample of meteorites available for study, helping us understand the limitations in using this sample to draw conclusions about the broader meteoroid population impacting Earth.

## METHODS

### Meteorites with Instrumentally Measured Orbits

To examine biases in the population of meteorite falls with known orbits, we compiled a data set of 75 meteorites with instrumentally measured trajectories. These “orbital meteorites” span over six decades, from the first recorded case of Příbram in 1959 (Ceplecha, 1961) to recent recoveries such as Ribbeck in 2024 (Spurný, Caffee, et al., 2024). The masses of recovered meteorites in this dataset vary widely, from fragments of tens of grams to the > 1000 kg recovered after the Chelyabinsk impact (Popova et al., 2013).

The 75 recovered orbital meteorites used in this study are listed in Table 1. A majority of the trajectory data come from peer-reviewed articles; however, several of the meteorite orbits were obtained from abstracts, proceedings, and preliminary processing.

### The Fireball Data

This study utilizes data from three major fireball observation networks: the EN, FRIPON, and GFO. These networks specialize in detecting and recording fireball events and have been instrumental in recovering meteorites with associated orbital data.

The European Fireball Network (EN; <https://meteor.asu.cas.cz/en/en/>), established in 1963, is the longest-running fireball observation network and has significantly advanced our understanding of meteoroid dynamics and meteorite recovery (Borovička et al., 2022). The EN utilizes a network of 21 Digital Autonomous Fireball Observers (DAFOs) equipped with DSLR cameras and fisheye lenses to capture fireball trajectories over an approximately 1 million square kilometer coverage area of the sky across Central Europe. The German portion of the network’s operation concluded in 2022, leaving the Czech Republic and Slovakia as the primary regions hosting the DAFO systems. These

systems can detect meteors brighter than magnitude  $-2$  and perform radiometric measurements on those brighter than magnitude  $-4$ . The EN employs a straight-line least squares (SLLS) method for trajectory reconstruction (Borovička, 1990), incorporating atmospheric models such as CIRA72 and NRLMSISE-00 to refine calculations (Borovička et al., 2022). This enables the precise determination of meteoroid trajectories, including pre-atmospheric velocities, and the estimation of terminal masses using a physical four-parameter velocity model. The EN fireball data used here was taken from Borovička et al. (2022), which describes 824 fireballs observed by the EN between 2017 and 2018.

FRIPON (<https://www.fripon.org/>; Fireball Recovery and InterPlanetary Observation Network), operational since 2015, spans a coverage area exceeding 2 million square kilometers across Europe and neighboring regions, with over 250 wide-field cameras and 40 radio receivers (Colas et al., 2020). The wide-angle CCD cameras record at 30 frames per second, producing high-time-resolution data. The detections and underlying data are available on the consortium webpage (<https://fireball.fripon.org>). The limiting magnitude of any single frame is  $\sim 0$ , but longer exposures are taken every 10 min to acquire better astrometry and photometry, resulting in a good signal-to-noise ratio (S/N) up to a stellar magnitude of 6 for dark sites (Anghel et al., 2019; Colas et al., 2020; Jeanne, 2020; Jeanne et al., 2019). The network’s automation and open-access model produces a rapid response for meteorite recovery campaigns. The FRIPON fireball data used here is a subset of data collected between 2016 and 2023.

The Global Fireball Observatory (<https://gfo.rocks/>; GFO) is a global collaboration utilizing the long-exposure photographic hardware and GNSS-synchronized liquid crystal shutters to track fireball events (Devillepoix et al., 2020). The GFO’s extensive coverage area, precise manually reduced observations, and the multidisciplinary team have been instrumental to the successful recovery of at least 16 meteorites (<https://dfn.gfo.rocks/meteorites.html>) to date. The GFO project was initiated by members of the Desert Fireball Network (DFN), and the hardware and software utilized by all partner networks were originally developed for the DFN (Howie, Paxman, Bland, Towner, Cupak, et al., 2017; Howie, Paxman, Bland, Towner, Sansom, et al., 2017; Sansom et al., 2015; Sansom, Jansen-Sturgeon, et al., 2019). The GFO utilizes high-resolution DSLR cameras paired with all-sky fisheye lenses. The observatories exhibit a limiting magnitude of 0 for fireballs and 4 for astrometry, allowing the capture of meteoroids as small as approximately 5 cm while they are still at higher altitudes before significant atmospheric deceleration occurs. The GFO data examined in this study stem from observations taken between 2014 and 2023.

TABLE 1. 75 recovered meteorite falls used in this study. Falls with only preliminary, unpublished values available were taken from Jenniskens and Devillepoix (2025).

Name	Type	Location	Date	$m_{\infty}$ (kg)	$m_{found}$ (kg)	Source
Pribram	H5	Czech Rep.	1959/04/07	< 5000	5.56	Ceplecha (1961)
Lost City	H5	USA	1970/01/04	165	17	McCrosky et al. (1971)
Ischgl	LL6	Czech Rep.	1970/11/24	130	0.71	Gritsevich et al. (2024)
Innisfree	L5	Canada	1977/02/06	42	4.58	Halliday et al. (1978)
Benešov	LL3.5, H5	Czech Rep.	1991/05/07	4100	0.01	Spurný et al. (2014)
Peekskill	H6	USA	1992/10/09	< 10,000	12.57	Brown et al. (1994)
Tagish Lake	C2-ung.	Canada	2000/01/18	75,000	10	Brown et al. (2000)
Moravka	H5	Czech Rep.	2000/05/06	1500	0.63	Borovička and Kalenda (2003)
Neuschwanstein	EL6	Germany	2002/04/06	300	6.19	Spurný et al. (2003)
Park Forest	L5	USA	2003/03/27	11,000	18	Brown et al. (2004)
Villalbeto de la Peña	L6	Spain	2004/01/04	760	3.5	Llorca et al. (2005)
Bunburra Rockhole	Eurcite	Australia	2007/07/20	22	0.32	Bland et al. (2009)
Almahata Sitta	Ureilite + other	Sudan	2008/10/07	83,000	3.95	Jenniskens et al. (2009)
Buzzard Coulee	H4	Canada	2008/11/21	15,000	41	Fry et al. (2013)
Maribo	CM2	Denmark	2009/01/17	1500	0.03	Borovička et al. (2019)
Jesenice	L6	Slovenia	2009/04/09	170	3.67	Spurný et al. (2010)
Grimsby	H5	Canada	2009/09/26	33	0.22	Brown et al. (2011)
Kosice	H5	Slovakia	2010/02/28	3500	4.3	Borovička, Tóth, et al. (2013)
Mason Gully	H5	Australia	2010/04/13	40	0.02	Dyl et al. (2016)
Mifflin	L5	USA	2010/04/15	1000	3.58	Kita et al. (2013)
Križevci	H6	Croatia	2011/02/04	25–100	0.29	Borovička, Spurný, Šegon, et al. (2015)
Sutter's Mill	C, CM2	USA	2012/04/22	50,000	0.99	Jenniskens et al. (2012)
Novato	L6	USA	2012/10/18	80	0.31	Jenniskens et al. (2014)
Chelyabinsk	LL5	Russia	2013/02/15	1,200,000	1000?	Popova et al. (2013)
Benghazi Dam	H5	Australia	2013/07/31	7900	> 4	Preliminary results, unpublished in journals
Annama	H5	Russia	2014/04/18	472	0.17	Kohout et al. (2017)
Žďár nad Sázavou	L3	Czech Rep.	2014/12/09	170	0.05	Spurný et al. (2020)
Porangaba	L4	Brazil	2015/01/09	0.976	0.976	Ferus et al. (2020)
Sarıçiçek	Howardite	Turkey	2015/09/02	6000–20,000	15.24	Unsalan et al. (2019)
Creston	L6	USA	2015/10/24	10–100	0.688	Jenniskens et al. (2019)
Murrili	H5	Australia	2015/10/27	37.9±2.3	1.68	Sansom et al. (2020)
Osceola	L6	USA	2016/01/24	> 1800	1.099	Gritsevich et al. (2017)
Ejby	H5/6	Denmark	2016/02/06	250	8.94	Spurný et al. (2017)
Stubenberg	LL6	Germany	2016/03/06	600.0	1.47	Preliminary results, unpublished in journals
Hradec Králové	LL5	Czech Rep.	2016/05/17	90.0	0.134	Preliminary results, unpublished in journals
Dishchii'bikoh	LL7	USA	2016/06/02	3000–15,000	0.0795	Jenniskens et al. (2020)
Dingle Dell	L/LL5	Australia	2016/10/31	40	1.15	Devillepoix et al. (2018)
Crawford Bay	H6	Canada	2017/09/05	2500.0	-	Preliminary results, unpublished in journals
Hamburg	H4	USA	2018/01/17	60–225	1	Brown et al. (2019)
Motopi Pan	Howardite	Botswana	2018/06/02	5500	0.214	Jenniskens et al. (2021)
Ozerki	L6	Russia	2018/06/21	94,000±20,000	6.5	Kartashova et al. (2020)
Renchen	L5-6	Germany	2018/07/10	17.0	0.999	Preliminary results, unpublished in journals
Arpu Kuilpu	H5	Australia	2019/06/01	0.91	0.031	Shober et al. (2022)
Aguas Zarcas	CM2	Costa Rica	2019/04/24	300.0	27	Jenniskens et al. (2025)

TABLE 1. *Continued.* 75 recovered meteorite falls used in this study. Falls with only preliminary, unpublished values available were taken from Jenniskens and Devillepoix (2025).

Name	Type	Location	Date	$m_{\infty}$ (kg)	$m_{found}$ (kg)	Source
Viñales	L6	Cuba	2019/02/01	—	50	Zuluaga et al. (2019)
Flensburg	C1-ungr.	Germany	2019/09/12	10,000–20,000	0.0245	Borovička, Bettonvil, et al. (2021)
Puli Ilkaringuru	H5	Australia	2019/11/18	—	0.369	Preliminary results, unpublished in journals
Cavezzo	L5-an	Italy	2020/01/01	3.5	0.055	Gardiol et al. (2021)
Novo Mesto	L5	Slovenia	2020/02/28	470	0.72	Vida et al. (2021)
Tiros	Howardite	Brazil	2020/05/08	240.0	0.4	Preliminary results, unpublished in journals
Madura Cave	L5	Australia	2020/06/19	30–60	1.072	Devillepoix et al. (2022)
Narashino	H5	Japan	2020/07/02	—	0.35	Preliminary results, unpublished in journals
Santa Filomena	H5-6	Brazil	2020/09/19	—	80	Tosi et al. (2023)
Ådalen	Iron	Sweden	2020/11/07	8500.0	13.8	Kyrylenko et al. (2023)
Kindberg	L6	Austria	2020/11/19	270	0.233	Ferriere et al. (2022)
Traspena	L5	Spain	2021/01/18	2620	0.527	Andrade et al. (2023)
Winchcombe	CM2	UK	2021/02/28	12.5	0.602	McMullan et al. (2024)
Kybo-Lintos	H4-5	Australia	2021/04/01	—	0.07	Preliminary results, unpublished in journals
Antonin	L5	Poland	2021/07/15	50–500	0.35	Shrbený et al. (2022)
Taghzout	H5	Morocco	2021/05/06	—	2.1	Preliminary results, unpublished in journals
Golden	L/LL5	Canada	2021/10/04	70	2.2	Brown et al. (2023)
Al-Khadhaf	H5-6	Oman	2022/03/08	0.6	0.0221	Preliminary results, unpublished in journals
Pusté Úlany	H5	Slovakia	2022/06/25	50.0	0.0086	Preliminary results, unpublished in journals
Great Salt Lake	H5	USA	2022/08/13	—	3.466	Preliminary results, unpublished in journals
Junction City	L5	USA	2022/09/26	25.0	1.951	Preliminary results, unpublished in journals
Tanxi	H6	China	2022/12/15	—	10.7	Preliminary results, unpublished in journals
Mvskoke Merkv	L6	USA	2023/01/20	—	1.421	Preliminary results, unpublished in journals
Saint-Pierre-le-Viger	L5-6	France	2023/02/13	780	1.2	Egal et al. (2025)
Matera	H5	Italy	2023/02/14	10.0	0.1175	Preliminary results, unpublished in journals
Elmshorn	H3-6	Germany	2023/04/25	180.0	4.28	Preliminary results, unpublished in journals
Ménétréol-sur-Sauldre	H5	France	2023/09/09	3.5	0.714	Preliminary results, unpublished in journals
Raja	EH3	Oman	2023/12/23	0.4	0.0268	Preliminary results, unpublished in journals
La Posa Plain	LL3-6	USA	2023/12/29	2	0.565	Preliminary results, unpublished in journals
Ribbeck	Aubrite	Germany	2024/01/24	140	1.8	Spurný, Borovička, et al. (2024)
Takapō	L5	New Zealand	2024/03/13	1.0	0.81	Preliminary results, unpublished in journals

### Identification of Meteorite Falls

For the EN data set, the estimated terminal masses were calculated according to the methodology outlined

by Borovička et al. (2022). This approach involves applying a four-parameter physical velocity model to the entire meteoroid trajectory, assuming a shape-density coefficient of  $\Gamma A = 0.7$  and a meteoroid density of



$\rho_d = 3000 \text{ kg m}^{-3}$ . Mass estimates are provided only for meteoroids with terminal masses of at least 1 g and terminal velocities below  $10 \text{ km s}^{-1}$ ; otherwise, the mass is considered negligible.

For FRIPON and GFO data, we employed the  $\alpha$ - $\beta$  criterion as described by Sansom, Gritsevich, et al. (2019) to identify potential meteorite falls. This method calculates two key parameters: the ballistic coefficient ( $\alpha$ ), related to the meteoroid's mass and drag characteristics, and the mass-loss parameter ( $\beta$ ), which quantifies the extent of mass loss during atmospheric entry. Values of  $\alpha$  and  $\beta$  are calculated using least-squares minimization of the analytical function (see section 3 of Lyytinen & Gritsevich, 2016, after Gritsevich, 2007). Plotting these parameters on an  $\alpha$ - $\beta$  diagram allows us to distinguish meteorite-dropping events based on their deceleration behavior (see section 2 of Sansom, Gritsevich, et al., 2019).

By solving equation 6 in Sansom, Gritsevich, et al. (2019) for a final mass of  $M_f = 1 \text{ g}$ , we used a meteoroid density of  $\rho_d = 2400 \text{ kg m}^{-3}$  and a typical shape-drag coefficient,  $c_{dA} = 1.5$  (Gritsevich, 2008), to get a value of  $\ln(M_f/M_0)^* = -17.1$ . We can plot this boundary, as done in figures 3 and 4 in Sansom, Gritsevich, et al. (2019), given the two extremes for the shape change parameter  $\mu = 0$  (i.e., there is no spin of the meteoroid), and when  $\mu = 2/3$  (i.e., sufficient spin for equal ablation over the entire meteoroid surface and no shape change is expected to occur):

$$\ln(\beta) = \ln(17.1 - 3\ln(\alpha \sin \gamma)), \quad \mu = 0, \quad (1)$$

$$\ln(\beta) = \ln(5.7 - \ln(\alpha \sin \gamma)), \quad \mu = \frac{2}{3}, \quad (2)$$

where  $\gamma$  is the meteoroid's entry angle, and  $\mu$  represents the shape change coefficient (ranging from 0 to  $\frac{2}{3}$ ) indicating meteoroid rotation.

To estimate final masses *quantitatively*, certain assumptions are necessary regarding parameters like the drag coefficient ( $C_d$ ), initial cross-sectional area ( $S_0$ ), initial shape coefficient ( $A_0$ ), and meteoroid bulk density ( $\rho_m$ ). The atmospheric surface density ( $\rho_0$ ) is typically set to  $1.21 \text{ kg m}^{-3}$ . While these assumptions are common across various methods, the parameters in this approach are generally confined within well-established ranges due to extensive documentation of meteoroid densities, shape coefficients, and drag values. Importantly, using the  $\alpha$ - $\beta$  meteorite-dropping methodology circumvents the need for uncertain ablation parameters and luminous efficiency estimates, the two parameters with the highest uncertainties (Loehle et al., 2024). Rearranging equation 2 in Sansom, Gritsevich, et al. (2019) for  $\alpha$  demonstrates that meteoroids with varying entry masses, angles, and volumes can yield similar  $\alpha$  values, making  $\alpha$  and  $\beta$  robust

predictors of atmospheric entry outcomes compared to traditional parameter sets.

For a comprehensive understanding of the  $\alpha$ - $\beta$  methodology and its applications, we refer readers to Gritsevich and Stulov (2006); Gritsevich (2007, 2009); Gritsevich et al. (2011); Gritsevich et al. (2012); Sansom, Gritsevich, et al. (2019); Boaca et al. (2022). The  $\alpha$  and  $\beta$  parameters can be calculated for any event with available velocity and altitude data and  $>80\%$  deceleration profiles, aiding in the assessment of meteorite survivability ([https://github.com/desertfireballnetwork/alpha\\_beta\\_modules](https://github.com/desertfireballnetwork/alpha_beta_modules)). Recently, a complementary differential-evolution based methodology has also been developed by Peña-Asensio and Gritsevich (2025) to derive  $\alpha$ - $\beta$  along with other parameters using legacy or incomplete data sets.

### Initial Mass Estimations

Both EN and FRIPON publish photometric entry masses. The EN method is described, and the data is available in Borovička et al. (2022). Meanwhile, the FRIPON photometric mass estimation method estimates the radiative output  $I_0$  as defined in Ceplecha et al. (1998), and the radiated energy was converted into source energy using the relation derived by Anghel et al. (2021). For a general overview of both methods, please refer to section 3.2 of Shober, Devillepoix, et al. (2025). The GFO, in contrast, adopts an Extended Kalman Smoother (EKS) that fits the single-body deceleration equations and therefore yields a dynamic entry mass (Sansom et al., 2015). While the model used by the EKS does not explicitly account for fragmentation, the data reflects both effects of ablation and fragmentation, and the EKS assimilates every new position measurement. Any unmodeled impulse, such as a sudden deceleration caused by fragmentation, appears as an increase in the magnitude of the state variance matrix  $P_k$  and is absorbed into the process-noise term. The subsequent update step reallocates mass from the state vector, so the filter steps down the main-body mass exactly at fragmentation epochs without the need to pre-define fragment events (Sansom et al., 2015). Recent work has shown that even greater fidelity can be obtained by fitting the deceleration and light curve simultaneously; although this increases the number of free parameters, it yields a more complete history of mass loss (Borovička et al., 2020; Vida et al., 2024).

To test whether the mixed photometric–dynamic catalogue used here could bias our mass bins, we also examined the thousands of sporadic fireballs observed by FRIPON for which dynamic and photometric masses are calculated for each event (Anghel et al., 2019; Colas et al., 2020; Jeanne et al., 2019). Among 1492 such fireballs the median absolute difference  $\Delta M = |M_{\text{phot}} - M_{\text{dyn}}|$  is

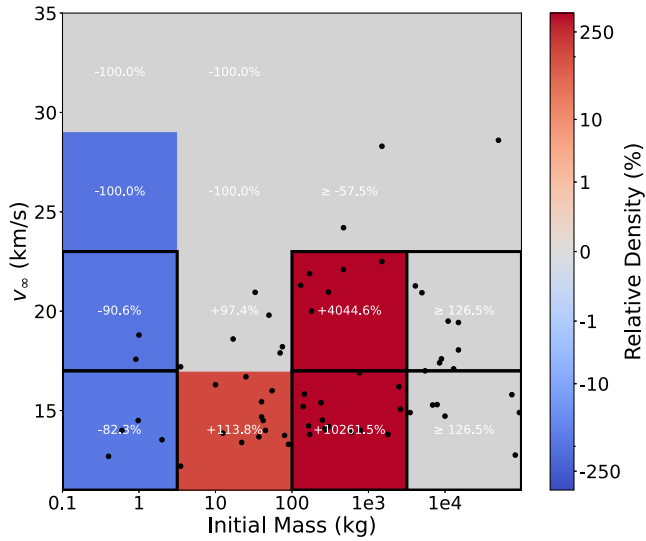


FIGURE 1. Density heatmaps comparing the relative distribution of 75 meteorite falls with instrumentally measured orbits to possible  $\geq 1$  g meteorite falls (538 impacts) for initial mass (kg) versus the initial velocity at the top of the atmosphere ( $\text{km s}^{-1}$ ). The colors represent relative density differences, calculated as the percentage change between the two populations. Red regions represent regions overrepresented in the recovered meteorite, and blue regions are where we should have more meteorites recovered. The statistical significance of the differences was determined using a chi-squared test for each bin, with black borders highlighting regions with significance at the  $3\sigma$  level and all other colored bins having a  $2\sigma$  level.

0.26 kg (0.1–1 kg), 1.38 kg (1–10 kg), and 17.2 kg (10–100 kg). Fig. 1 employs only four bins (0.1–5 kg, 5–100 kg, 100–5000 kg, and 5000–100,000 kg). Even the most significant offsets reported by Lyytinen and Gritsevich (2016) or by our FRIPON observations cannot shift an event across a bin boundary.

### Observational Biases

Before proceeding, it is essential to acknowledge the observational biases inherent in photographic and video fireball networks. These biases include:

- Night only observation bias (i.e., the antihelion direction).
- Seasonal weather observation variations.
- Seasonal Day/night length variation.
- Lunar-related minimum camera sensitivity cycle.
- Speed bias at minimum observational magnitudes.
- Earth's gravitational focusing increases the proportion of slow-impactors.

Out of these biases, the most prevalent to consider is the speed bias for faint meteors, which generally increases

the proportion of larger semi-major axis orbits within an impacting data set. However, since this study only focuses on bright, meteorite-dropping fireballs, this bias is not present in this subset of EN/FRIPON/GFO events. This is because the limiting magnitude of each camera system is much more sensitive than the faintest meteorite-dropping fireball event. Meanwhile, the other biases listed above related to annual or monthly variations also do not affect the results of this study. While these effects, particularly seasonal weather, can drastically modify the distributions of solar longitudes, the velocity distributions and  $a-e-t$  distribution do not vary. There is evidence that very minor variations exist in the  $\lambda_{\odot}$  or  $\Omega$  distributions of NEAs (JeongAhn & Malhotra, 2014); however, there is zero correlation between  $a-e-t$  and  $\lambda_{\odot}$  or  $\Omega$ . Gravitational focusing likewise affects both the potential-fall and recovered-fall samples equally, and thus divides out in the relative density comparison. Consequently, while no ground-based survey is fully unbiased, the specific selection effects above do not compromise the recovery bias signal we quantify in sections 3–4.

### Analysis of Orbital Distribution and Statistical Assessment

To quantitatively compare the distributions, we constructed two-dimensional histograms of paired orbital elements such as semi-major axis ( $a$ ) versus eccentricity ( $e$ ),  $a$  versus inclination ( $i$ ),  $i$  versus perihelion distance ( $q$ ), and  $i$  versus aphelion distance ( $Q$ ). We also created a similar 2D histogram of initial velocity versus initial mass to test our hypothesis that meteorite recovery efforts are significantly biased toward slower and larger falls. The parameter space was adequately covered by dividing each orbital element into either 4 or 9 bins ( $2 \times 2$  or  $3 \times 3$  grid). Meanwhile, the velocity–mass plane was divided into four equal-width bins in log mass, so that the bin widths exceed the typical photometric-vs-dynamic mass offsets described in “Initial Mass Estimations” Section. Sensitivity checks were performed, ranging from four to 100 total bins. Within each bin, we counted the number of meteoroids from the reference population (538 possible meteorite-dropping fireballs) and the subset population (the 75 recovered meteorites with orbits). Given that  $\alpha \propto M_e^{-1}$  and  $\beta \propto V_e^2$  (Gritsevich, 2007, 2009), binning our events by  $\log M_e$  and  $V_e$  is analogous to binning by  $\ln \alpha$  and  $\ln \beta$  (Gritsevich et al., 2011, 2012). This analytical link demonstrates that the mass- and velocity-selection effects arise directly from first principles; the subsequent Fisher's test serve only as an independent quantitative check and a means to understand the magnitude of the bias.

To test whether the recovered fraction differs from the reference fraction in each cell  $(i, j)$  we apply Fisher's exact test (two-sided) to the  $2 \times 2$  table

$$\begin{bmatrix} \text{recovered in} & \text{recovered out} \\ \text{reference in} & \text{reference out} \end{bmatrix} = \begin{bmatrix} a_{ij} & c_{ij} \\ b_{ij} & d_{ij} \end{bmatrix},$$

which yields a  $p$ -value  $p_{ij}$  for the null hypothesis of equal in-cell probabilities (Agresti & Kateri, 2011).

However, as multiple cells are tested simultaneously, per-cell  $p$ -values are adjusted using the Benjamini–Hochberg false discovery rate (FDR) procedure (Benjamini & Hochberg, 1995). Let  $q_{ij}$  denote the BH-adjusted  $p$ -value ( $q$ -value) for cell  $(i, j)$ . Unless otherwise stated, a cell is considered significant if  $q_{ij} \leq 0.05$ . For visual emphasis we additionally mark cells that reach approximately  $3\sigma$  evidence, defined as  $p_{ij} < 0.0027$  (two-sided), with a solid black border. Cells that reached  $2\sigma$  significance ( $p_{ij} < 0.0455$ ) are colored but have no border.

To quantify the disparity between the populations, we calculated the relative difference in normalized densities for each bin. Let  $p_{ij}^{\text{ref}} = b_{ij}/N_{\text{ref}}$  and  $p_{ij}^{\text{rec}} = a_{ij}/N_{\text{rec}}$  be the in-cell probabilities for the two samples. We report the per-cell relative change (percent excess/deficit) as

$$\Delta_{ij} = 100 \frac{p_{ij}^{\text{rec}} - p_{ij}^{\text{ref}}}{p_{ij}^{\text{ref}}}. \quad (3)$$

Normalization was achieved by dividing the count in each bin by the total number of meteoroids in the corresponding population.

When  $b_{ij} = 0$  ( $p_{ij}^{\text{ref}} = 0$ ), the ratio in Equation (3) is undefined and we color the cell gray. If such a cell is nevertheless statistically significant by Fisher's test and FDR, we report a conservative one-sided lower confidence bound on the relative risk  $RR_{ij} = p_{ij}^{\text{rec}}/p_{ij}^{\text{ref}}$  computed from one-sided Clopper–Pearson bounds (lower bound for  $p_{ij}^{\text{rec}}$ , upper bound for  $p_{ij}^{\text{ref}}$ ) and present it as a minimum percent change,  $100(RR_{ij, \text{lower}} - 1)$ , displayed as “ $\geq \%$ ” inside the cell. The one-sided tail probability is matched to the evidence level (e.g., 0.02275 for “ $2\sigma$ ” and 0.00135 for “ $3\sigma$ ”), ensuring the bound is at least as stringent as the significance threshold.

Density heatmaps (Figures 1 and 2) were generated to visualize the relative differences across the orbital parameter spaces. The color scale represented the value of  $\Delta$ , utilizing a symmetric logarithmic normalization to highlight both positive and negative variations. Bins with statistically significant differences were accentuated—those significant at the  $3\sigma$  level were marked with bold borders, while those at the  $2\sigma$  level have no border. Only bins that reach at least the  $2\sigma$  level of significance are shown in Figures 1 and 2.

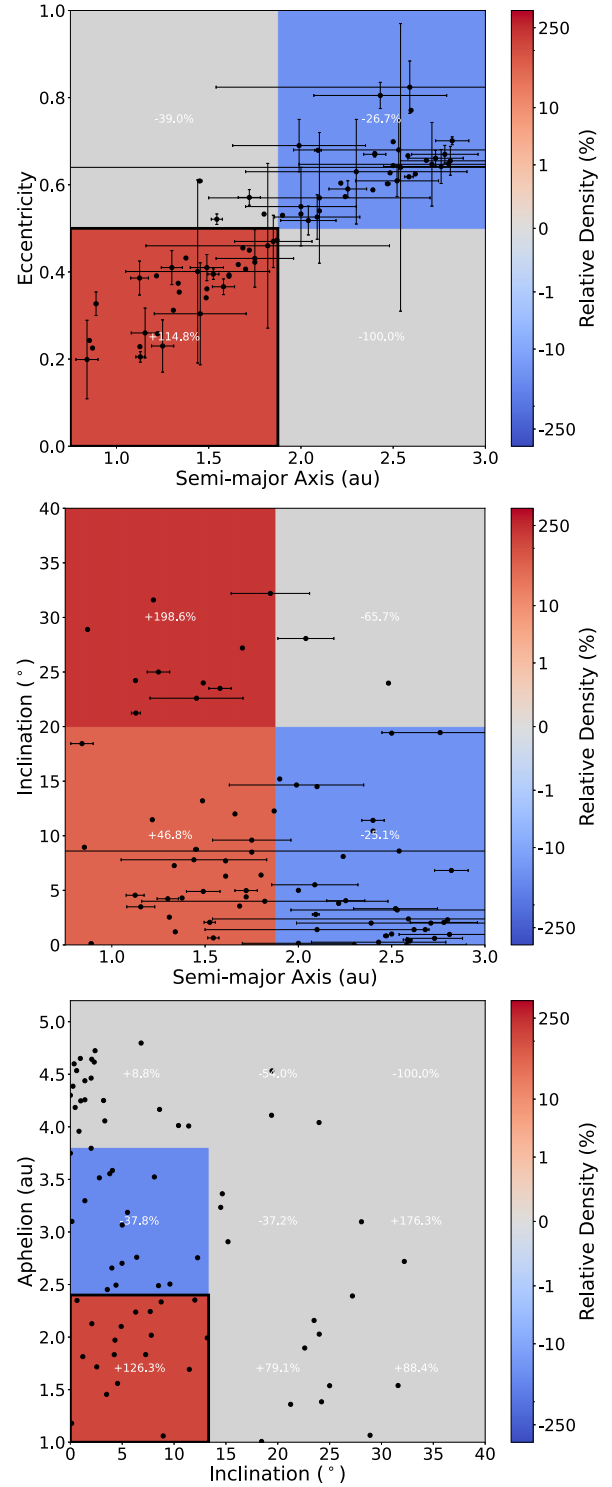


FIGURE 2. Density heatmaps comparing the distribution of 75 recovered meteorite falls (with measured orbits) to 538 potential  $\geq 1$  g falls across semi-major axis vs eccentricity, semi-major axis versus inclination, and inclination vs aphelion distance. Colors show relative density differences (red = overrepresented, blue = underrepresented). Black borders indicate  $3\sigma$  significance; all other colored bins are at least  $2\sigma$ . The 75 recovered orbits appear as black points.



## RESULTS

### What Are We Searching For?

Our analysis began by examining the characteristics of meteorites that are most commonly targeted for recovery efforts. Figure 1 displays a density heatmap comparing the distribution of initial masses and velocities of the 75 orbital meteorites to a data set of 538 potential meteorite falls (with estimated final masses  $\geq 1$  g) identified by the EN, FRIPON, and GFO networks. The color scale represents the relative density differences between the two populations, where a degree of significance of at least  $2\text{-}\sigma$  is reached.

The results indicate a significant bias toward larger meteoroids with lower entry velocities in the recovered sample. Given that the ballistic coefficient ( $\alpha$ ) is inversely proportional to the meteoroid's initial mass  $M_e^{-1}$ , and the mass-loss parameter ( $\beta$ ) scales with the square of the entry velocity  $V_e^2$ , the  $\alpha$ - $\beta$  space is effectively a mass-velocity phase diagram: large, slow bodies plot at low- $\alpha$  and low- $\beta$ , precisely where atmospheric filtering predicts successful meteorite falls (Gritsevich et al., 2011, 2012). Our statistical tests here simply quantify and validate that physically expected skew with observational data.

Meteoroids estimated to have initial masses  $> 100$  kg and pre-atmospheric velocities  $< 22.5$  km s $^{-1}$  are extremely disproportionately represented among the recovered falls by 4000–10,000% (approximately 40–100 $\times$ ). It is important to note that although this observation is extremely significant, the exact magnitude of the bias remains uncertain due to low counting statistics. This trend reflects the practical considerations of meteorite recovery: larger meteoroids are more likely to survive atmospheric entry and produce larger fragments that can be found on the ground. Meanwhile, slower entry velocities reduce ablation and fragmentation, thereby increasing the chances of recovery. Conversely, smaller meteoroids ( $\leq 10$  kg) at low to medium entry velocities are underrepresented in the recovered sample at rates around  $-80\%$  to  $-90\%$  relative to the expected deposition rate (blue bins in Figure 1).

### How Do Our Biases Affect the Orbits?

To evaluate the impact of our recovery biases on the observed orbital distribution of meteorites with known orbits, we compared the orbital parameters of the 75 recovered meteorites to those of the 538 potential meteorite-dropping fireballs detected by the EN, FRIPON, and GFO networks. Figure 2 presents density heatmaps showing the relative differences between these two populations across various orbital parameter spaces, including semi-major axis versus eccentricity, semi-major

axis versus inclination, inclination versus perihelion distance, and inclination versus aphelion distance.

Figure 2 reveals a clear  $+100\%$ – $200\%$  (corresponding to proportionally  $2\text{--}3\times$  more) excess of recovered meteorites originating from orbits with semi-major axes less than 1.8 au, which corresponds to the orbits outside of the range of the main belt on evolved orbits closer to the Earth. These findings show that meteorites from the evolved orbits are around  $\sim 2\text{--}3\times$  more likely to be recovered compared to the falls from the main belt due to low-velocity search bias. This bias against would be especially true for those samples originating from the outer main belt.

## DISCUSSION

Our analysis quantifies the well-known tendency of fall searches to favor slow and large meteoroids, as lower-velocity meteoroids are more likely to survive atmospheric entry and produce recoverable fragments (Ceplecha et al., 1998). The underlying physics is apparent in the  $\ln\alpha$ - $\ln\beta$  plane, where  $\alpha \propto M_e^{-1}$  and  $\beta \propto V_e^2$  (Gritsevich, 2007, 2009; Gritsevich et al., 2011, 2012; Sansom, Gritsevich, et al., 2019). The lower-left quadrant marks the region where atmospheric survival is most probable (cf. figure 4 of Sansom, Gritsevich, et al., 2019).

Consistent with this expectation, our recovered meteorite set exhibits a  $\sim 2\text{--}3\times$  excess of orbits originating in the inner main belt and highly evolved orbits, specifically those with semi-major axes  $a \lesssim 1.8$  au (Figure 2). These bodies are primarily being delivered by the  $\nu_6$  resonance (Bottke Jr. et al., 2002; Granvik et al., 2018; Greenstreet et al., 2012; Nesvorný et al., 2023; Nesvorný, Vokrouhlický, Shelly, Deienno, Bottke, Christensen, et al., 2024; Nesvorný, Vokrouhlický, Shelly, Deienno, Bottke, Fuls, et al., et al., 2024). Thus, indicating we are overpredicting the magnitude delivered from the  $\nu_6$  when only considering instrumentally observed meteorite falls.

The recovered meteorite set is also subject to a pronounced mass bias: meteorites derived from impactors  $\geq 100$  kg are 40–100 $\times$  more prevalent than expected based on observed possible falls (Figure 1). If the intrinsic orbital distribution of meteoroids were nearly independent of size, this bias would merely rescale the recovered masses. In reality, several size-dependent processes (e.g., collisional comminution, thermal cracking, micrometeoroid erosion, etc.) can imprint different orbital signatures on centimeter, meter, and decameter bodies. For example, impacts detected by U.S. government (USG) sensors (<https://cneos.jpl.nasa.gov/fireballs/>) are the largest impactors hitting the Earth, and they overwhelmingly tend to have a concentration at  $a < 2$  au (i.e., the inner-belt delivery route; Brown et al., 2016; Chow & Brown, 2025). If this

distribution is accurate, it suggests that the overabundance of recoveries at lower semi-major axis values in our sample could also be influenced by our mass bias, where larger impactors are more likely to originate from lower semi-major axis values relative to smaller meteoroids. However, caution is warranted, as the CNEOS data set lacks formal velocity uncertainties (Brown & Borovička, 2023; Devillepoix et al., 2019; Hajdukova et al., 2024). Recent calibration against 18 events with independent ground-based solutions shows the USG/CNEOS orbits split cleanly into two accuracy regimes: for fireballs reported after late-2017 or with impact energies  $\geq 0.45$  kt, typical agreement is  $D_D \approx 0.03 \pm 0.02$  and 74%–78% of cases satisfy  $D_D < 0.1$ , whereas older/low-energy events are much less reliable (Peña-Asensio et al., 2025). Thus, the orbital distribution derived from USG sensors should be viewed with skepticism. Decameter-sized NEAs observed telescopically also tend to have lower semi-major axis values compared to decameter Earth impactors (Chow & Brown, 2025), but this is likely due to observational bias (Jedicke et al., 2016; Nesvorný et al., 2023). The lower semi-major axis values of large impactors cannot be related to tidal disruption (or other mechanisms) in recent history ( $< 10$  kyrs; Shober, Courtot, et al., 2024; Chow & Brown, 2025) or a longer-term tidal signature (based on the  $q$ -distribution; Chow & Brown, 2025). A more plausible contributor potentially is the progressive breakup of weak, particularly carbonaceous NEAs, where thermal fragmentation and small impacts continuously inject meter-scale fragments into near-Earth space (Shober, Caffee, et al., 2024; Shober, Devillepoix, et al., 2025). Such fresh debris would enhance the local flux of large meteoroids without forming coherent streams, consistent with the negative results of dedicated stream searches (Koten et al., 2014; Pauls & Gladman, 2005; Reddy et al., 2015; Shober, 2025; Shober, Courtot, et al., 2024). Determining exactly how these fragmentation processes reshape the size-dependent orbital distribution will require new models of the centimeter- to decameter-scale meteoroid environment. Developing and validating those models is an important task for future work.

We also examined how the searches distort the recovered fragment-size distribution of the orbital meteorites. Figure 3 compares the cumulative size-frequency distribution (SFD) of fragments reported from 51 orbital meteorite falls (black curve) with the well-searched strewn fields of several falls and also ANSMET meteorites. This juxtaposition was made to provide a comparison to the less-biased fragment data sets of well-searched strewn fields and ANSMET Antarctic finds. The overall SFD of fragments from the fireball-recovered meteorites (black curve) shows a slight deviation from the Antarctic SFD at smaller fragment sizes ( $< 100$  g), indicating an expected reduced recovery

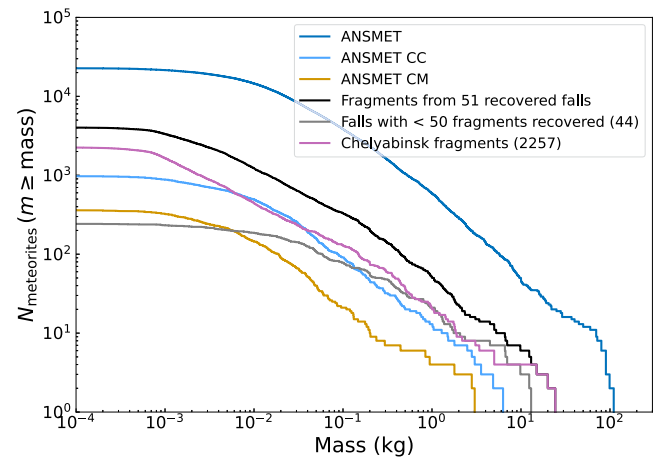


FIGURE 3. Cumulative size-frequency distribution (SFD) for recovered meteorite fragments from 51 of the “orbital meteorites” versus the Antarctic meteorites recovered by the US-led Antarctic Search for Meteorites program (ANSMET).

rate for smaller fragments. However, this deviation is not pronounced, primarily because the overall fragment SFD is heavily influenced by a small number of large, well-searched strewn fields, such as the Almahata Sitta fall (over 600 fragments; Shaddad et al., 2010), the Sariççek fall (343 fragments; Unsalan et al., 2019), and the recent Ribbeck aubrite fall (nearly 200 fragments; Bischoff et al., 2024), which together account for over half of all fragments in our data set, excluding Chelyabinsk. The Chelyabinsk fall (pink curve) produced over 2000 fragments (2257 included here) (Brykina & Egorova, 2024; Popova et al., 2013). Following the fragment count of Brykina and Egorova (2024), we include the 24.3 kg stone identified by local historians and later documented by Kolisnichenko (2019) as the video-tracked fragment F2 of Borovička, Spurný, et al. (2013), together with four still-unrecovered pieces (5–20 kg) predicted by the same fragmentation model (extended data figure 6: Borovička, Spurný, et al., 2013). To better understand the general characteristics of smaller falls and smaller, less extensive recovery efforts, we also plot the SFD for falls with fewer than 50 fragments (gray curve; Figure 3). This curve reveals a much steeper divergence from the Antarctic SFD and well-recovered falls, with a recovery bias that starts to deviate from linear significantly below fragment sizes of 500 g. This pattern highlights the challenges of recovering small fragments (such as those in challenging terrains, dense vegetation, etc.), which are compounded by our bias toward search efforts that typically prioritize larger initial impactors, as they are more likely to produce recoverable samples.

This recovery bias has broader implications for source region analyses, particularly for meteoroid populations

that produce smaller fragments upon atmospheric entry. Carbonaceous chondrites, for instance, are disproportionately affected by this bias. Over 90% of all ANSMET carbonaceous chondrites (light-blue curve; Figure 3) are <90 g, and 90% of ANSMET CM carbonaceous chondrites (orange curve; Figure 3) are <50 g. During atmospheric entry, carbonaceous chondrites undergo more continuous fragmentation, producing a higher proportion of smaller fragments relative to ordinary chondrites (Borovička et al., 2019, 2020). Within the ANSMET collection, the median meteorite mass is 18 g, whereas the median mass of a carbonaceous chondrite is 10 and 7 g for CMs. Carbonaceous falls seem to produce many more fragments within the 1–10 g range; however, it isn't easy to quantify. Even for the Antarctic collection, fragments <50–100 g tend to be significantly transported by wind, greatly increasing their likelihood of being removed from the search locations rapidly (Cassidy et al., 1992; Harvey, 1995; Schutt et al., 1986). Given our inherent recovery bias against smaller fragments, it is likely that falls of small carbonaceous meteoroids, similar to Winchcombe (estimated initial mass  $\approx 13$  kg), are among the most underrepresented in our samples. This is further corroborated by the fact that four out of five carbonaceous chondrite falls recovered with known orbits were exceptionally large, with pre-entry masses often exceeding tens of thousands of kilograms (Borovička et al., 2019; Borovička, Betttonvil, et al., 2021; Brown et al., 2000; Jenniskens et al., 2012; King et al., 2022).

While the ideal solution would be to recover more meteorites with a broader range of entry velocities and initial masses, doing so is inherently challenging. Even with dedicated efforts, locating small meteorite falls remains a challenging task, and search missions are limited by practical constraints (e.g., funding, terrain complexities). Nonetheless, advancements in observational technologies, trajectory modeling, and targeted search strategies, including the use of drones and machine learning, are increasingly allowing us to detect and recover smaller and more diverse events (Anderson et al., 2020, 2022; Citron et al., 2021). We have already demonstrated success with objects with initial masses as small as a few kilograms (Gardiol et al., 2021; Shober et al., 2022; Zappatini et al., 2024), suggesting that continued innovation in search techniques can further mitigate these biases. In any case, if wanting to use orbital meteorites to constrain meteorite families and source regions, search bias effects need to be accounted for.

## CONCLUSIONS

Our study quantified the biases in the population of recovered meteorites with known orbits. These biases

stem from the practical challenges and methodologies associated with meteorite recovery efforts, resulting in a pronounced overrepresentation of larger, slower-moving meteoroids. Our analysis quantifies these biases in the subset of meteorites with instrumentally constrained trajectories:

1. *Orbital bias*: falls originating on inner-belt evolved orbits ( $a \lesssim 1.8$  au) are recovered  $2-3\times$  more frequently than their occurrence rate among 538 potential GFO/EN/FRIPON meteorite-droppers.
2. *Mass bias*: entry masses  $M_{\infty} \gtrsim 100$  kg are favored by  $40-100\times$  (due to low statistics in these bins, the exact magnitude of the bias is very uncertain), whereas  $M_{\infty} \lesssim 10$  kg bodies are underrepresented by 80%–90%.

An intriguing consideration is the potential mass-dependent variation in the orbital distribution of impactors. If larger impactors tend to have lower semi-major axes, as U.S. Government sensor detections suggest, the overabundance of recoveries from lower semi-major axis values could be partially due to mass-dependent orbital variation. The effect of these biases results in overstating the contribution of the  $\nu_6$  resonance and undersampling weak, carbonaceous material. In any case, some recovery bias is unavoidable, and we must take it into account when using recovered meteorite falls with instrumentally measured orbits to constrain contributions from the meteorite source regions.

**Acknowledgments**—Research was sponsored by the National Aeronautics and Space Administration (NASA) through a contract with ORAU. The views and conclusions contained in this document are those of the authors and should not be interpreted as representing the official policies, either expressed or implied, of the NASA or the US Government. The US Government is authorized to reproduce and distribute reprints for Government purposes notwithstanding any copyright notation herein. This project has received funding from the European Union's Horizon 2020 research and innovation programme under the Marie Skłodowska-Curie grant agreement no. 945298. The Global Fireball Observatory and data pipeline is enabled by the support of the Australian Research Council (DP230100301, LE170100106). FRIPON was initiated by funding from ANR (grant N.13-BS05-0009-03), carried by the Paris Observatory, Muséum National d'Histoire Naturelle, Paris-Saclay University and Institut Pythéas (LAM-CEREGE). VigieCiel was part of the 65 Millions d'Observateurs project, carried by the Muséum National d'Histoire Naturelle and funded by the French Investissements d'Avenir program. FRIPON data are hosted and processed at Institut Pythéas SIP (Service



Informatique Pythéas), and a mirror is hosted at IMCCE (Institut de Mécanique Céleste et de Calcul des Éphémérides/Paris Observatory). The authors would also like to thank Maria Gritsevich and an anonymous reviewer for their thoughtful reviews leading to many improvements within the manuscript.

**Data Availability Statement**—The data that support the findings of this study are available from the corresponding author upon reasonable request.

**Editorial Handling**—Dr. Josep M. Trigo-Rodríguez

## REFERENCES

- Agresti, A., & Kateri, M. 2011 *International Encyclopedia of Statistical Science*, 206–8. Heidelberg, Germany: Springer.
- Anderson, S., Towner, M., Bland, P., Haikings, C., Volante, W., Sansom, E., Devillepoix, H., et al. 2020. Machine Learning for Semi-Automated Meteorite Recovery. *Meteoritics & Planetary Science* 55: 2461–71.
- Anderson, S. L., Towner, M. C., Fairweather, J., Bland, P. A., Devillepoix, H. A. R., Sansom, E. K., Cupák, M., Shober, P. M., and Benedix, G. K. 2022. Successful Recovery of an Observed Meteorite Fall Using Drones and Machine Learning. *The Astrophysical Journal Letters* 930: L25.
- Andrade, M., Docobo, J. Á., García-Guinea, J., Campo, P. P., Tapia, M., Sánchez-Muñoz, L., Villasante-Marcos, V., et al. 2023. The Traspensa Meteorite: Heliocentric Orbit, Atmospheric Trajectory, Strewn Field, and Petrography of a New L5 Ordinary Chondrite. *Monthly Notices of the Royal Astronomical Society* 518: 3850–76.
- Anghel, S., Birlan, M., Nedelcu, D.-A., and Boaca, I. 2019. Photometric Calibration of Moroi All-Sky Cameras: Introduction and First Results. *Romanian Astronomical Journal* 29: 191.
- Anghel, S., Drolshagen, E., Ott, T., Birlan, M., Colas, F., Nedelcu, D. A., Koschny, D., et al. 2021. Energy Signature of Ton TNT-Class Impacts: Analysis of the 2018 December 22 Fireball over Western Pyrenees. *Monthly Notices of the Royal Astronomical Society* 508: 5716–33. <https://doi.org/10.1093/mnras/stab2968>.
- Ashimbekova, A., Vaubaillon, J., and Koten, P. 2025. Towards a Definition of a Meteor Cluster. *Astronomy & Astrophysics* 696: A69.
- Benjamini, Y., and Hochberg, Y. 1995. Controlling the False Discovery Rate: A Practical and Powerful Approach to Multiple Testing. *Journal of the Royal Statistical Society, Series B: Statistical Methodology* 57: 289–300.
- Bischoff, A., Patzek, M., Barrat, J.-A., Berndt, J., Busemann, H., Degering, D., di Rocco, T., et al. 2024. Cosmic Pears from the Havelland (Germany): Ribbeck, the Twelfth Recorded Aubrite Fall in History. *Meteoritics & Planetary Science* 59: 2660–94.
- Bland, P. A., Spurný, P., Towner, M. C., Bevan, A. W., Singleton, A. T., Bottke, Jr W. F., Greenwood, R. C., et al. 2009. An Anomalous Basaltic Meteorite from the Innermost Main Belt. *Science* 325: 1525–27.
- Boaca, I., Gritsevich, M., Birlan, M., Nedelcu, A., Boaca, T., Colas, F., Malgouyre, A., Zanda, B., and Vernazza, P. 2022. Characterization of the Fireballs Detected by all-Sky Cameras in Romania. *The Astrophysical Journal* 936: 150.
- Bockelee-Morvan, D., Biver, N., Moreno, R., Colom, P., Crovisier, J., Gérard, É., Henry, F., et al. 2001. Outgassing Behavior and Composition of Comet C/1999 S4 (LINEAR) During its Disruption. *Science* 292: 1339.
- Borovička, J. 1990. The Comparison of Two Methods of Determining Meteor Trajectories from Photographs. *Astronomical Institutes of Czechoslovakia, Bulletin* 41: 391–96.
- Borovička, J., Bettonvil, F., Baumgarten, G., Strunk, J., Hankey, M., Spurný, P., and Heinlein, D. 2021. Trajectory and Orbit of the Unique Carbonaceous Meteorite Flensburg. *Meteoritics & Planetary Science* 56: 425–439.
- Borovička, J., and Kalenda, P. 2003. The Morávka Meteorite Fall: 4. Meteoroid Dynamics and Fragmentation in the Atmosphere. *Meteoritics & Planetary Science* 38: 1023–43.
- Borovička, J., Popova, O., and Spurný, P. 2019. The MariboCM2 Meteorite Fall—Survival of Weak Material at High Entry Speed. *Meteoritics & Planetary Science* 54: 1024–41.
- Borovička, J., Spurný, P., and Brown, P. 2015. Asteroids IV, 257.
- Borovička, J., Spurný, P., Brown, P., Wiegert, P., Kalenda, P., Clark, D., Shrubbený, L., et al. 2013. The Trajectory, Structure and Origin of the Chelyabinsk Asteroidal Impactor. *Nature* 503: 235–37.
- Borovička, J., Spurný, P., Šegon, D., Andreić, Ž., Kac, J., Korlević, K., Atanackov, J., et al. 2015. The Instrumentally Recorded Fall of the Križevci Meteorite, Croatia, February 4, 2011. *Meteoritics & Planetary Science* 50: 1244–59.
- Borovička, J., Spurný, P., and Shrubbený, L. 2020. Two Strengths of Ordinary Chondritic Meteoroids as Derived from their Atmospheric Fragmentation Modeling. *Astronomical Journal* 160: 42.
- Borovička, J., Spurný, P., Shrubbený, L., Štork, R., Kotková, L., Fuchs, J., Kečliková, J., Zichová, H., Mánek, J., Váchová, P., Macourková, I. 2022. Data on 824 Fireballs Observed by the Digital Cameras of the European Fireball Network in 2017–2018-i. Description of the Network, Data Reduction Procedures, and the Catalog. *Astronomy & Astrophysics* 667: A157.
- Borovička, J., Tóth, J., Igaz, A., Spurný, P., Kalenda, P., Haloda, J., Svoreň, J., et al. 2013. The Košice Meteorite Fall: Atmospheric Trajectory, Fragmentation, and Orbit. *Meteoritics & Planetary Science* 48: 1757–79.
- Bottke, W. F., Jr., Morbidelli, A., Jedicke, R., Petit, J.-M., Levison, H. F., Michel, P., and Metcalfe, T. S. 2002. Debaised Orbital and Absolute Magnitude Distribution of the Near-Earth Objects. *Icarus* 156: 399.
- Bottke, W. F., Nolan, M. C., Greenberg, R., and Kolvoord, R. A. 1994. Collisional Lifetimes and Impact Statistics of Near-Earth Asteroids. In *Hazards Due to Comets and Asteroids*, edited by T. Gehrels, M. S. Matthews, and A. Schumann, 337. Tucson, AZ: University of Arizona Press.
- Brown, P., Ceplecha, Z., Hawkes, R., Hawkes, R. L., Wetherill, G., Beech, M., and Mossman, K. 1994. The Orbit and Atmospheric Trajectory of the Peekskill Meteorite from Video Records. *Nature* 367: 624–26.
- Brown, P., McCausland, P., Fries, M., Silber, E., Edwards, W. N., Wong, D. K., Weryk, R. J., Fries, J., and Krzeminski, Z. 2011. The Fall of the Grimsby Meteorite—I: Fireball Dynamics and Orbit from Radar, Video, and Infrasound Records. *Meteoritics & Planetary Science* 46: 339–363.



- Brown, P., Pack, D., Edwards, W., Edwards, W. N., Revelle, D. O., Yoo, B. B., Spalding, R. E., and Tagliaferri, E. 2004. The Orbit, Atmospheric Dynamics, and Initial Mass of the Park Forest Meteorite. *Meteoritics & Planetary Science* 39: 1781–96.
- Brown, P., Wiegert, P., Clark, D., and Tagliaferri, E. 2016. Orbital and Physical Characteristics of Meter-Scale Impactors from Airburst Observations. *Icarus* 266: 96–111.
- Brown, P. G., and Borovička, J. 2023. On the Proposed Interstellar Origin of the USG 20140108 Fireball. *ApJ* 953: 167.
- Brown, P. G., Hildebrand, A. R., Zolensky, M. E., Grady, M., Clayton, R. N., Mayeda, T. K., Tagliaferri, E., et al. 2000. The Fall, Recovery, Orbit, and Composition of the Tagish Lake Meteorite: A New Type of Carbonaceous Chondrite. *Science* 290: 320–25.
- Brown, P. G., McCausland, P., Hildebrand, A., Hanton, L. T. J., Eckart, L. M., Busemann, H., Krietsch, D., et al. 2023. The Golden Meteorite Fall: Fireball Trajectory, Orbit, and Meteorite Characterization. *Meteoritics & Planetary Science* 58: 1773.
- Brown, P. G., Vida, D., Moser, D., Moser, D. E., Granvik, M., Koshak, W. J., Chu, D., et al. 2019. The Hamburg Meteorite Fall: Fireball Trajectory, Orbit, and Dynamics. *Meteoritics & Planetary Science* 54: 2027–45.
- Brož, M., Vernazza, P., Marsset, M., Binzel, R. P., DeMeo, F., Birlan, M., Colas, F., et al. 2024. Source Regions of Carbonaceous Meteorites and near-Earth Objects. *Astronomy & Astrophysics* 689: A183.
- Brož, M., Vernazza, P., Marsset, M., DeMeo, F. E., Binzel, R. P., Vokrouhlický, D., and Nesvorný, D. 2024. Young Asteroid Families as the Primary Source of Meteorites. *Nature* 634: 566–571.
- Brykina, I., and Egorova, L. 2024. Describing the Fragment Mass Distribution in Meteorite Showers. *Planetary and Space Science* 241: 105838.
- Cambioni, S., Delbo, M., Poggiali, G., Avdellidou, C., Ryan, A. J., Deshapriya, J. D. P., Asphaug, E., et al. 2021. Fine-Regolith Production on Asteroids Controlled by Rock Porosity. *Nature* 598: 49–52.
- Čapek, D., Koten, P., Spurný, P., and Shrbený, L. 2022. Ejection Velocities, Age, and Formation Process of SPE Meteoroid Cluster. *Astronomy & Astrophysics* 666: A144.
- Čapek, D., and Vokrouhlický, D. 2010. Thermal Stresses in Small Meteoroids. *Astronomy & Astrophysics* 519: A75.
- Čapek, D., and Vokrouhlický, D. 2012. Thermal Stresses in Small Meteoroids. *Astronomy & Astrophysics* 539: A25.
- Cassidy, W., Harvey, R., Schutt, J., Delisle, G., and Yanai, K. 1992. The Meteorite Collection Sites of Antarctica. *Meteoritics* 27: 490–525.
- Cepplecha, Z. 1961. *Bulletin of the Astronomical*, Vol. 12. 21. Prague, Czechoslovakia: Institute of Czechoslovakia.
- Cepplecha, Z., Borovička, J., Elford, W. G., ReVelle, D. O., Hawkes, R. L., Porubčan, V. Í., and Šimek, M. 1998. Meteor Phenomena and Bodies. *Space Science Reviews* 84: 327–471.
- Chow, I., and Brown, P. G. 2025. Decameter-Sized Earth Impactors—I: Orbital Properties. *Icarus* 429: 116444.
- Citron, R. I., Jenniskens, P., Watkins, C., Sinha, S., Shah, A., Raissi, C., Devillepoix, H., and Albers, J. 2021. Recovery of Meteorites Using an Autonomous Drone and Machine Learning. *Meteoritics & Planetary Science* 56: 1073–85.
- Colas, F., Zanda, B., Bouley, S., Jeanne, S., Malgouyre, A., Birlan, M., Blanpain, C., et al. 2020. FRIPON: A Worldwide Network to Track Incoming Meteoroids. *Astronomy and Astrophysics* 644: A53.
- Corrigan, C. M., Welzenbach, L. C., Righter, K., McBride K. M., McCoy T. J., Harvey R. P., Satterwhite C. E. 2014. 35 Seasons of US Antarctic Meteorites (1976–2010) *A Pictorial Guide to the Collection*, 173. Washington, D.C: American Geophysical Union.
- Delbo, M., Libourel, G., Wilkerson, J., Murdoch, N., Michel, P., Ramesh, K. T., Ganino, C., Verati, C., and Marchi, S. 2014. Thermal Fatigue as the Origin of Regolith on Small Asteroids. *Nature* 508: 233–36.
- Devillepoix, H. A., Bland, P. A., Sansom, E. K., Devillepoix, H. A. R., Towner, M. C., Cupák, M., Howie, R. M., Hartig, B. A. D., Jansen-Sturgeon, T., and Cox, M. A. 2019. Observation of Metre-Scale Impactors by the Desert Fireball Network. *Monthly Notices of the Royal Astronomical Society* 483: 5166–78.
- Devillepoix, H. A., Sansom, E. K., Bland, P. A., Devillepoix, H. A. R., Towner, M. C., Cupák, M., Howie, R. M., et al. 2018. The Dingle Dell Meteorite: A Halloween Treat from the Main Belt. *Meteoritics & Planetary Science* 53: 2212–27.
- Devillepoix, H. A. R., Cupák, M., Bland, P. A., Sansom, E. K., Towner, M. C., Howie, R. M., Hartig, B. A. D., et al. 2020. A Global Fireball Observatory. *Planetary and Space Science* 191: 105036.
- Devillepoix, H. A. R., Sansom, E. K., Shober, P., Anderson, S. L., Towner, M. C., Lagain, A., Cupák, M., et al. 2022. Trajectory, Recovery, and Orbital History of the Madura Cave Meteorite. *Meteoritics & Planetary Science* 57: 1328. <https://doi.org/10.1111/maps.13820>.
- Dyl, K. A., Benedix, G. K., Bland, P. A., Friedrich, J. M., Spurný, P., Towner, M. C., O’Keefe, M. C., et al. 2016. Characterization of Mason Gully (H5): The Second Recovered Fall from the Desert Fireball Network. *Meteoritics & Planetary Science* 51: 596–613.
- Egal, A., Vida, D., Colas, F., Zanda, B., Bouley, S., Steinhäusser, A., Vernazza, P., et al. Catastrophic Disruption of Asteroid 2023 CX1 and Implications for Planetary Defence. *Nat Astron* (2025). <https://doi.org/10.1038/s41550-025-02659-8>
- Farinella, P., Vokrouhlický, D., and Hartmann, W. K. 1998. Meteorite Delivery via Yarkovsky Orbital Drift. *Icarus* 132: 378–387.
- Ferriere, L., Roszjar, J., and Povinec, P. 2022. The Kindberg L6 Ordinary Chondrite Fall and Recovery in Austria-A Case Study of Citizen Science. *85th Annual Meeting of The Meteoritical Society* 85: 6116.
- Ferus, M., Petera, L., Koukal, J., Lenža, L., Drtinová, B., Haloda, J., Matýšek, D., et al. 2020. Elemental Composition, Mineralogy and Orbital Parameters of the Porangaba Meteorite. *Icarus* 341: 113670.
- Fry, C., Melanson, D., Samson, C., McCausland, P. J. A., Herd, R. K., Ernst, R. E., Umoh, J., and Holdsworth, D. W. 2013. Physical Characterization of a Suite of Buzzard Coulee H4 Chondrite Fragments. *Meteoritics & Planetary Science* 48: 1060–73.
- Gardioli, D., Barghini, D., Buzzoni, A., Carbognani, A., Di Carlo, M., Di Martino, M., Knapic, C., et al. 2021. Cavezzo, the First Italian Meteorite Recovered by the PRISMA Fireball Network. Orbit, Trajectory, and Strewn-field. *Monthly Notices of the Royal Astronomical Society* 501: 1215.
- Granvik, M., Morbidelli, A., Jedicke, R., Bolin, B., Bottke, W. F., Beshore, E., Vokrouhlický, D., Delbò, M., and Michel, P.

2016. Super-Catastrophic Disruption of Asteroids at Small Perihelion Distances. *Nature* 530: 303–6.
- Granvik, M., Morbidelli, A., Jedicke, R., Bolin, B., Bottke, W. F., Beshore, E., Vokrouhlický, D., Nesvorný, D., and Michel, P. 2018. Debaised Orbit and Absolute-Magnitude Distributions for near-Earth Objects. *Icarus* 312: 181–207.
- Greenstreet, S., Ngo, H., and Gladman, B. 2012. The Orbital Distribution of Near-Earth Objects Inside Earth's Orbit. *Icarus* 217: 355–366.
- Gritsevich, M. 2009. Determination of Parameters of Meteor Bodies Based on Flight Observational Data. *Advances in Space Research* 44: 323–334.
- Gritsevich, M., Lyytinen, E., and Hankey, M. 2017. European Planetary Science Congress, EPSC2017–995.
- Gritsevich, M., Moilanen, J., Visuri, J., Meier, M. M. M., Maden, C., Oberst, J., Heinlein, D., et al. 2024. The Fireball of November 24, 1970, as the Most Probable Source of the Ischgl Meteorite. *Meteoritics & Planetary Science* 59: 1658–91.
- Gritsevich, M., and Stulov, V. 2006. Extra-Atmospheric Masses of the Canadian Network Bolides. *Solar System Research* 40: 477–484.
- Gritsevich, M., Stulov, V., and Turchak, L. 2012. Consequences of Collisions of Natural Cosmic Bodies with the Earth's Atmosphere and Surface. *Cosmic Research* 50: 56–64.
- Gritsevich, M. I. 2007. Approximation of the Observed Motion of Bolides by the Analytical Solution of the Equations of Meteor Physics. *Solar System Research* 41: 509–514. <https://doi.org/10.1134/S003809460706007X>.
- Gritsevich, M. I. 2008. Validity of the Photometric Formula for Estimating the Mass of a Fireball Projectile. *Physics-Doklady* 53: 97–102. <https://doi.org/10.1134/S1028335808020110>.
- Gritsevich, M. I., Stulov, V. P., and Turchak, L. I. 2011. Standards for Crater Formation and Meteorite Fallout by the Light Sector of an Atmospheric Trajectory. *Physics-Doklady* 56: 199–203. <https://doi.org/10.1134/S1028335811030116>.
- Hajdukova, M., Stober, G., Barghini, D., Koten, P., Vaubaillon, J., Sterken, V. J., Ďurišová, S., Jackson, A., Desch, S. 2024. No Evidence for Interstellar Fireballs in the CNEOS Database. *Astronomy & Astrophysics* 691: A8.
- Halliday, I., Blackwell, A. T., and Griffin, A. A. 1978. Detailed Records of Many Unrecovered Meteorites in Western Canada for Which Further Searches Are Recommended. *Journal of the Royal Astronomical Society of Canada* 72: 15–39.
- Harvey, R. 1995. Workshop on Meteorites from Cold and Hot Deserts, 34.
- Harvey, R. 2003. The Origin and Significance of Antarctic Meteorites. *Geochemistry* 63: 93–147.
- Howie, R. M., Paxman, J., Bland, P. A., C. Towner, M., Cupak, M., Sansom, E. K., and A. R. Devillepoix, H. 2017. How to Build a Continental Scale Fireball Camera Network. *Experimental Astronomy* 43: 237–266.
- Howie, R. M., Paxman, J., Bland, P. A., Towner, M. C., Sansom, E. K., and Devillepoix, H. A. R. 2017. Submillisecond Fireball Timing Using de Bruijn Timecodes. *Meteoritics & Planetary Science* 52: 1669–82.
- Jeanne, S. 2020. PhD Thesis, Université Paris sciences et lettres.
- Jeanne, S., Colas, F., Zanda, B., Birlan, M., Vaubaillon, J., Bouley, S., Vernazza, P., et al. 2019. Calibration of Fish-Eye Lens and Error Estimation on Fireball Trajectories: Application to the FRIPON Network. *Astronomy and Astrophysics* 627: A78.
- Jedicke, R., Bolin, B., Granvik, M., and Beshore, E. 2016. A Fast Method for Quantifying Observational Selection Effects in Asteroid Surveys. *Icarus* 266: 173–188.
- Jenniskens, P., and Devillepoix, H. A. 2025. Review of Asteroid, Meteor, and Meteorite-Type Links. *Meteoritics & Planetary Science* 60: 928–973.
- Jenniskens, P., Fries, M. D., Yin, Q.-Z., Zolensky, M., Krot, A. N., Sandford, S. A., Sears, D., et al. 2012. Radar-Enabled Recovery of the Sutter's Mill Meteorite, a Carbonaceous Chondrite Regolith Breccia. *Science* 338: 1583–87.
- Jenniskens, P., Gabadirewe, M., Yin, Q.-Z., Proyer, A., Moses, O., Kohout, T., Franchi, F., et al. 2021. The Impact and Recovery of Asteroid 2018 LA. *Meteoritics & Planetary Science* 56: 844–893.
- Jenniskens, P., Moskovitz, N., Garvie, L. A., Garvie, L. A. J., Yin, Q.-Z., Howell, J. A., Free, D. L., et al. 2020. Orbit and Origin of the LL 7 Chondrite Dishchii'bikoh (Arizona). *Meteoritics & Planetary Science* 55: 535–557.
- Jenniskens, P., Rubin, A. E., Yin, Q.-Z., Sears, D. W. G., Sandford, S. A., Zolensky, M. E., Krot, A. N., et al. 2014. Fall, Recovery, and Characterization of the Novato L6 Chondrite Breccia. *Meteoritics & Planetary Science* 49: 1388–1425.
- Jenniskens, P., Soto, G. J., Goncalves Silva, G., Lücke, O., Madrigal, P., Ballester, T., Salas Matamoros, C., et al. 2025. Orbit, Meteoroid Size, and Cosmic Ray Exposure History of the Aguas Zarcas CM2 breccia. *Meteoritics & Planetary Science* 60: 997–1022.
- Jenniskens, P., Uras, J., Yin, Q.-Z., Matson, R. D., Fries, M., Howell, J. A., Free, D., et al. 2019. The Creston, California, Meteorite Fall and the Origin of L Chondrites. *Meteoritics & Planetary Science* 54: 699–720.
- Jenniskens, P. A., Shaddad, M. H., Numan, D., Jenniskens, P., Elsir, S., Kudoda, A. M., Zolensky, M. E., et al. 2009. The Impact and Recovery of Asteroid 2008 TC3. *Nature* 458: 485–88.
- JeongAhn, Y., and Malhotra, R. 2014. On the Non-Uniform Distribution of the Angular Elements of near-Earth Objects. *Icarus* 229: 236–246.
- Kartashova, A., Golubaev, A., Mozgova, A., Chuvashov, I., Bolgova, G., Glazachev, D., and Efremov, V. 2020. Investigation of the Ozerki Meteoroid Parameters. *Planetary and Space Science* 193: 105034.
- King, A. J., Daly, L., Rowe, J., Joy, K. H., Greenwood, R. C., Devillepoix, H. A., Suttle, M. D., et al. 2022. The Winchcombe Meteorite, a Unique and Pristine Witness from the Outer Solar System. *Science Advances* 8: eabq3925. <https://doi.org/10.1126/sciadv.abq3925>.
- Kita, N. T., Welten, K. C., Valley, J. W., Spicuzza, M. J., Nakashima, D., Tenner, T. J., Ushikubo, T., et al. 2013. Fall, Classification, and Exposure History of the Mifflin L5 Chondrite. *Meteoritics & Planetary Science* 48: 641–655.
- Kohout, T., Haloda, J., Halodová, P., Meier, M. M. M., Maden, C., Busemann, H., Laubenstein, M., et al. 2017. Annama H Chondrite—Mineralogy, Physical Properties, Cosmic Ray Exposure, and Parent Body History. *Meteoritics & Planetary Science* 52: 1525–41.
- Kolishnichenko, S. V. 2019. *Meteorites of Russia: Sanarka, Chelyabinsk Region*. Russia: Chelyabinsk.
- Koten, P., Vaubaillon, J., Čapek, D., Vojáček, V., Spurný, P., Štork, R., and Colas, F. 2014. Search for Faint Meteors

- on the Orbits of Příbram and Neuschwanstein Meteorites. *Icarus* 239: 244–252.
- Kyrylenko, I., Golubov, O., Slyusarev, I., Visuri, J., Gritsevich, M., Krugly, Y. N., Belskaya, I., and Shevchenko, V. G. 2023. The First Instrumentally Documented Fall of an Iron Meteorite: Orbit and Possible Origin. *The Astrophysical Journal* 953: 20.
- Lauretta, D., Balram-Knutson, S., Beshore, E., Lauretta, D. S., Balram-Knutson, S. S., Boynton, W. V., Drouet d'Aubigny, C., et al. 2017. OSIRIS-REx: Sample Return from Asteroid (101955) Bennu. *Space Science Reviews* 212: 925–984.
- Llorca, J., Trigo-Rodríguez, J. M., Ortiz, J. L., Docobo, J. A., García-Guinea, J., Castro-Tirado, A. J., Rubin, A. E., et al. 2005. The Villalbeto de la Peña Meteorite Fall: I. Fireball Energy, Meteorite Recovery, Strewn Field, and Petrography. *Meteoritics & Planetary Science* 40: 795–804.
- Loehle, S., Vaubaillon, J., Matlovič, P., and Tóth, J. 2024. Meteorite Material Luminous Efficiencies from Ground Testing of Meteoroid Entry. *Icarus* 407: 115817.
- Lucchetti, A., Cambioni, S., Nakano, R., Barnouin, O. S., Pajola, M., Penasa, L., Tusberty, F., et al. 2024. Fast Boulder Fracturing by Thermal Fatigue Detected on Stony Asteroids. *Nature Communications* 15: 6206.
- Lyytinen, E., and Gritsevich, M. 2016. Implications of the Atmospheric Density Profile in the Processing of Fireball Observations. *Planetary and Space Science* 120: 35–42.
- Marsset, M., Vernazza, P., Brož, M., Thomas, C. A., DeMeo, F. E., Burt, B., Binzel, R. P., et al. 2024. The Massalia Asteroid Family as the Origin of Ordinary L Chondrites. *Nature* 634: 561–65.
- McCrosky, R. E., Posen, A., Schwartz, G., and Shao, C.-Y. 1971. Lost City Meteorite—its Recovery and a Comparison with Other Fireballs. *Journal of Geophysical Research* 76: 4090–4108.
- McMullan, S., Vida, D., Devillepoix, H. A., Devillepoix, H. A. R., Rowe, J., Daly, L., King, A. J., et al. 2024. The Winchcombe Fireball—That Lucky Survivor. *Meteoritics & Planetary Science* 59: 927–947.
- Molaro, J., Walsh, K., Jawin, E., Molaro, J. L., Walsh, K. J., Jawin, E. R., Ballouz, R.-L., et al. 2020. In Situ Evidence of Thermally Induced Rock Breakdown Widespread on Bennu's Surface. *Nature Communications* 11: 2913.
- Nesvorný, D., Deienno, R., Bottke, W. F., Jedicke, R., Naidu, S., Chesley, S. R., Chodas, P. W., et al. 2023. NEOMOD: A New Orbital Distribution Model for Near-Earth Objects. *The Astronomical Journal* 166: 55.
- Nesvorný, D., Vokrouhlický, D., Shelly, F., Deienno, R., Bottke, W. F., Christensen, E., Jedicke, R., et al. 2024. NEOMOD 2: An Updated Model of Near-Earth Objects from a Decade of Catalina Sky Survey Observations. *Icarus* 411: 115922.
- Nesvorný, D., Vokrouhlický, D., Shelly, F., Deienno, R., Bottke, W. F., Fuls, C., Jedicke, R., et al. 2024. NEOMOD 3: The Debaised Size Distribution of near Earth Objects. *Icarus* 417: 116110.
- Pauls, A., and Gladman, B. 2005. Decoherence Time Scales for “Meteoroid Streams”. *Meteoritics & Planetary Science* 40: 1241–56.
- Peña-Asensio, E., Grèbol-Tomás, P., Trigo-Rodríguez, J. M., Ramírez-Moreta, P., and Kresken, R. 2024. The 18 May 2024 Iberian Superbolide from a Sunskirting Orbit: USG Space Sensors and Ground-Based Independent Observations. *Monthly Notices of the Royal Astronomical Society: Letters* 533: L92–L99.
- Peña-Asensio, E., and Gritsevich, M. 2025. Inferring Fireball Velocity Profiles and Characteristic Parameters of Meteoroids from Incomplete Data Sets. *Journal of Geophysical Research: Planets* 130: e2024JE008382.
- Peña-Asensio, E., Socas-Navarro, H., and Seligman, D. Z. 2025. arXiv preprint arXiv:2508.01454.
- Popova, O. P., Jenniskens, P., Emel'yanenko, V., Kartashova, A., Biryukov, E., Khaibrakhmanov, S., Shuvalov, V., et al. 2013. Chelyabinsk Airburst, Damage Assessment, Meteorite Recovery, and Characterization. *Science* 342: 1069–73.
- Reddy, V., Vokrouhlický, D., Bottke, W. F., Pravec, P., Sanchez, J. A., Gary, B. L., Klima, R., et al. 2015. Link between the Potentially Hazardous Asteroid (86039) 1999 NC43 and the Chelyabinsk Meteoroid Tenuous. *Icarus* 252: 129–143.
- Rigley, J. K., and Wyatt, M. C. 2022. Comet Fragmentation as a Source of the Zodiacal Cloud. *Monthly Notices of the Royal Astronomical Society* 510: 834–857.
- Sansom, E. K., Bland, P., Paxman, J., and Towner, M. 2015. A Novel Approach to Fireball Modeling: The Observable and the Calculated. *Meteoritics & Planetary Science* 50: 1423–35.
- Sansom, E. K., Bland, P. A., Towner, M. C., Devillepoix, H. A. R., Cupák, M., Howie, R. M., Jansen-Sturgeon, T., et al. 2020. Murrili meteorite's Fall and Recovery from Kati Thanda. *Meteoritics & Planetary Science* 55: 2157–68.
- Sansom, E. K., Gritsevich, M., Devillepoix, H. A., Devillepoix, H. A. R., Jansen-Sturgeon, T., Shober, P., Bland, P. A., et al. 2019. Determining Fireball Fates Using the  $\alpha$ - $\beta$  Criterion. *The Astrophysical Journal* 885: 115.
- Sansom, E. K., Jansen-Sturgeon, T., Rutten, M. G., Devillepoix, H. A. R., Bland, P. A., Howie, R. M., Cox, M. A., Towner, M. C., Cupák, M., and Hartig, B. A. D. 2019. 3D Meteoroid Trajectories. *Icarus* 321: 388–406.
- Schutt, J., Schultz, L., Zinner, E., and Zolensky, M. 1986. Search for Meteorites in the Allan Hills Region, 1985–1986. *Antarctic Journal of the United States* 21: 82.
- Sekanina, Z., and Chodas, P. W. 2005. Origin of the Marsden and Kracht Groups of Sunskirting Comets. I. Association with Comet 96P/Machholz and its Interplanetary Complex. *The Astrophysical Journal Supplement Series* 161: 551–586.
- Sekanina, Z., and Chodas, P. W. 2007. Fragmentation Hierarchy of Bright Sungrazing Comets and the Birth and Orbital Evolution of the Kreutz System. II. The Case for Cascading Fragmentation. *The Astrophysical Journal* 663: 657–676.
- Sekanina, Z., and Chodas, P. W. 2012. Comet C/2011 W3 (Lovejoy): Orbit Determination, Outbursts, Disintegration of Nucleus, Dust-Tail Morphology, and Relationship to New Cluster of Bright Sungrazers. *The Astrophysical Journal* 757: 127.
- Shaddad, M. H., Jenniskens, P., Numan, D., Kudoda, A. M., Elsir, S., Riyad, I. F., Ali, A. E., et al. 2010. The Recovery of Asteroid 2008 TC3. *Meteoritics & Planetary Science* 45: 1557–89.
- Shestakova, L. I., Spasskyuk, R., and Omarov, C. 2025. Thermal Stresses as a Possible Mechanism for Initiating the Destruction of Comet Shoemaker–Levy 9. *Monthly Notices of the Royal Astronomical Society* 537: 2151–59.

- Shober, P. M. 2025. arXiv preprint arXiv:2508.08409 <https://arxiv.org/abs/2508.08409>.
- Shober, P. M., Caffee, M. W., and Bland, P. A. 2024. Cosmic-Ray Exposure Age Accumulated in near-Earth Space: A Carbonaceous Chondrite Case Study. *Meteoritics & Planetary Science* 59: 2695–2717. <https://doi.org/10.1111/maps.14246>.
- Shober, P. M., Courtot, A., and Vaubaillon, J. 2024. Near Earth Stream Decoherence Revisited: The Limits of Orbital Similarity. *Astronomy and Astrophysics* 693: A23. <https://arxiv.org/abs/2410.21585>.
- Shober, P. M., Devillepoix, H. A., Sansom, E. K., Devillepoix, H. A. R., Towner, M. C., Cupák, M., Anderson, S. L., et al. 2022. Arpu Kuilpu: An H5 from the Outer Main Belt. *Meteoritics & Planetary Science* 57: 1146.
- Shober, P. M., Devillepoix, H. A., Vaubaillon, J., Anghel, S., Deam, S. E., Sansom, E. K., Colas, F., Zanda, B., Vernazza, P., and Bland, P. 2025. Perihelion History and Atmospheric Survival as Primary Drivers of the Earth's Meteorite Record. *Nature Astronomy* 14:1–4.
- Shrbený, L., Krzesińska, A. M., Borovička, J., et al. 2022. Analysis of the Daylight Fireball of July 15, 2021, Leading to a Meteorite Fall and Find near Antonin, Poland, and a Description of the Recovered Chondrite. *Meteoritics & Planetary Science* 57: 2108–26.
- Spurný, P., Borovička, J., Baumgarten, G., Spurný, P., Tymiński, Z., and Kmiecik, K. 2017. Atmospheric Trajectory and Heliocentric Orbit of the Ejby Meteorite Fall in Denmark on February 6, 2016. *Planetary and Space Science* 143: 192–98.
- Spurný, P., Borovička, J., Kac, J., Kalenda, P., Atanackov, J., Kladnik, G., Heinlein, D., and Grau, T. 2010. Analysis of Instrumental Observations of the Jesenice Meteorite Fall on April 9, 2009. *Meteoritics & Planetary Science* 45: 1392–1407.
- Spurný, P., Borovička, J., and Shrbený, L. 2020. The Žďár nad Sázavou Meteorite Fall: Fireball Trajectory, Photometry, Dynamics, Fragmentation, Orbit, and Meteorite Recovery. *Meteoritics & Planetary Science* 55: 376–401.
- Spurný, P., Borovička, J., Shrbený, L., Hankey, M., and Neubert, R. 2024. Atmospheric Entry and Fragmentation of the Small Asteroid 2024 BX1: Bolide Trajectory, Orbit, Dynamics, Light Curve, and Spectrum. *Astronomy & Astrophysics* 686: A67.
- Spurný, P., Haloda, J., Borovička, J., Shrbený, L., and Halodová, P. 2014. Reanalysis of the Benešov Bolide and Recovery of Polymict Breccia Meteorites – Old Mystery Solved after 20 Years. *Astronomy & Astrophysics* 570: A39.
- Spurný, P., Oberst, J., and Heinlein, D. 2003. Photographic Observations of Neuschwanstein, a Second Meteorite from the Orbit of the Příbram Chondrite. *Nature* 423: 151–53.
- Tosi, A., Zucolotto, M. E., Andrade, D. P., Winter, O. C., Mourão, D. C., Sfai, R., Ziegler, K., et al. 2023. The Santa Filomena Meteorite Shower: Trajectory, Classification, and Opaque Phases as Indicators of Metamorphic Conditions. *Meteoritics & Planetary Science* 58: 621–642.
- Towner, M., Jansen-Sturgeon, T., Cupak, M., Towner, M. C., Sansom, E. K., Devillepoix, H. A. R., Bland, P. A., et al. 2022. Dark-Flight Estimates of Meteorite Fall Positions: Issues and a Case Study Using the Murrili Meteorite Fall. *The Planetary Science Journal* 3: 44.
- Unsalan, O., Jenniskens, P., Yin, Q.-Z., Kaygisiz, E., Albers, J., Clark, D. L., Granvik, M., et al. 2019. The Sariçiçek Howardite fall in Turkey: Source crater of HED meteorites on Vesta. *Meteoritics & Planetary Science* 54: 953–1008.
- Vida, D., Brown, P. G., Campbell-Brown, M., and Egal, A. 2024. First Holistic Modelling of Meteoroid Ablation and Fragmentation: A Case Study of the Orionids Recorded by the Canadian Automated Meteor Observatory. *Icarus* 408: 115842.
- Vida, D., Šegon, D., Šegon, M., et al. 2021. Novo Mesto Meteorite Fall–Trajectory, Orbit, and Fragmentation Analysis from Optical Observations. Technical Report, Copernicus Meetings.
- Watanabe, S.-I., Tsuda, Y., Yoshikawa, M., Tanaka, S., Saiki, T., and Nakazawa, S. 2017. Hayabusa2 Mission Overview. *Space Science Reviews* 208: 3–16.
- Wiegert, P., Brown, P., Pokorný, P., Ye, Q., Gregg, C., Lenartowicz, K., Krzeminski, Z., and Clark, D. 2020. Supercatastrophic Disruption of Asteroids in the Context of SOHO Comet, Fireball, and Meteor Observations. *The Astronomical Journal* 159: 143.
- Yoshikawa, M., Kawaguchi, J., Fujiwara, A., and Tsuchiyama, A. 2015. *Asteroids IV*. Tucson, Arizona: University of Arizona Press.
- Zappatini, A., Hofmann, B., Gnos, E., Eggenberger, U., Gfeller, F., and Kruttsch, P. M. 2024. Al-Khadhaf: A Camera-Observed H5-6 Fall from Oman. *LPI Contributions*, 3036, 6140.
- Zuluaga, J. I., Cuartas-Restrepo, P. A., Ospina, J., and Sucerquia, M. 2019. Can we Predict the Impact Conditions of Metre-Sized Meteoroids? *Monthly Notices of the Royal Astronomical Society: Letters* 486: L69–L73.